Eur. J. Mineral.
2005, **17**, 687-701

Magmatic garnet-bearing mafic xenoliths (Puy Beaunit, French Massif Central): P-T path from crystallisation to exhumation

Julien BERGER[1,2,*], Olivier FÉMÉNIAS[2], Nicolas COUSSAERT[3] and Daniel DEMAIFFE[2]

[1]Section de Géologie Isotopique, Musée Royal de l'Afrique centrale, B-3080 Tervuren, Belgium
[2]Laboratoire de Géochimie Isotopique et Géodynamique Chimique, DSTE, Université Libre de Bruxelles (CP 160/02), 50 Avenue Roosevelt, B-1050 Brussels, Belgium
[3]Unité de Géochimie et Minéralogie, Musée Royal de l'Afrique centrale, B-3080 Tervuren, Belgium

Abstract: Mafic xenoliths, sometimes interlayered with magmatic peridotites, are abundant in the scoria cones of Puy Beaunit in the French Massif Central. These are mainly layered gabbronorites with some norites, pyroxenites and anorthosites; they probably derive from a Permian differentiated deep layered intrusion. Crystallisation conditions were estimated at about 1000°C and 1 GPa. The rocks underwent sub-solidus re-equilibration at about 770°C and 1 GPa (isobaric cooling) in the lowermost crust. Two distinct symplectitic textures (pyroxene-plagioclase-spinel intergrowths) have been observed; they result from the destabilization of magmatic garnet (750-800°C, 0.55-0.8 GPa) and amphibole (990°C, < 0.3 GPa).

Melting of amphibole and destabilisation of orthopyroxene occurs during xenolith ascent. Garnet was destabilised either during tectonic uplift of the lower crust during Early Cenozoic or at the first step of xenolith ascent to the surface.

Whole-rock REE concentrations show that some xenoliths are typically plagioclase-rich cumulates, others are pyroxene-rich cumulates. Few mafic xenoliths display HREE enrichment, $(La/Yb)_N$ ratios lower than 1, presumably indicating garnet cumulation. Major-element composition of the fine-grained plagioclase-orthopyroxene-spinel symplectites is indeed close to that of a pyrope-almandine garnet with significant grossular content. The presence of this magmatic garnet argues for a hydrated calc-alkaline high-alumina basaltic magma in which the various mafic cumulates crystallised at depth.

Key-words: magmatic garnet; thermobarometry; mafic xenoliths; Puy Beaunit; pyrometamorphism; meta-cumulates.

Introduction

The Puy Beaunit Cenozoic volcano (Chaîne des Puys, French Massif Central) contains a wide range of xenoliths from both the upper mantle (mantle peridotites) and the crust (mafic-ultramafic meta-igneous xenoliths and meta-sedimentary xenoliths). Earlier works (*e.g.* Leyreloup, 1974; Downes *et al.*, 1991; Féménias *et al.*, 2003) have provided a petrological and geochemical overview of the xenoliths to better understand the evolution of the French Massif Central lithosphere through times. Féménias *et al.* (2003) have convincingly shown that mafic and ultramafic meta-cumulates from Beaunit are probably derived from a deep-seated layered intrusion.

Xenoliths of deep crustal origin are of great importance to understand the nature and evolution of the lower crust. It has been suggested (Downes *et al.*, 1991; Hermann *et al.*, 1997) that granulite-facies metamorphism can be induced by underplating of hot basaltic magma in the deep crust or at the crust-mantle boundary. Mafic xenoliths of meta-igneous origin can also be used to constrain the crystallisation history of basaltic magma at high pressure (around 1 GPa); this history may be quite different from basalt crystallisation at shallower levels, as shown by experimental studies (Green & Ringwood, 1968a; Nimis & Ulmer, 1998).

Moreover, xenoliths provide information about the effect of pyrometamorphism (HT-LP metamorphism of xenoliths during their rapid ascent to the surface in the host lava) on lower crustal rocks. Several types of effects can be observed: (1) infiltration of the host magma inside the xenolith inducing mineralogical and chemical changes (Faure *et al.*, 2001); (2) melting of some of the primary phases of the xenolith (Faure *et al.*, 2001; Braun & Kriegsman, 2001); (3) reactions between the primary phases to form coronitic and/or symplectitic textures (Berger & Forette, 1975) and (4) breakdown of primary phases under solid-state conditions (Mukhopadhyay, 1991). As a consequence of these effects, some primary phases can partially or totally disappear (ghost phases) and be replaced by associations of new, secondary mineral phases sometimes forming symplectitic intergrowths.

This paper presents a detailed petrological investigation of a suite of mafic xenoliths from Puy Beaunit (with new

*E-mail: julien.berger@africamuseum.be (J. Berger).

0935-1221/05/0017-0687 $ 6.75
DOI: 10.1127/0935-1221/2005/0017-0687

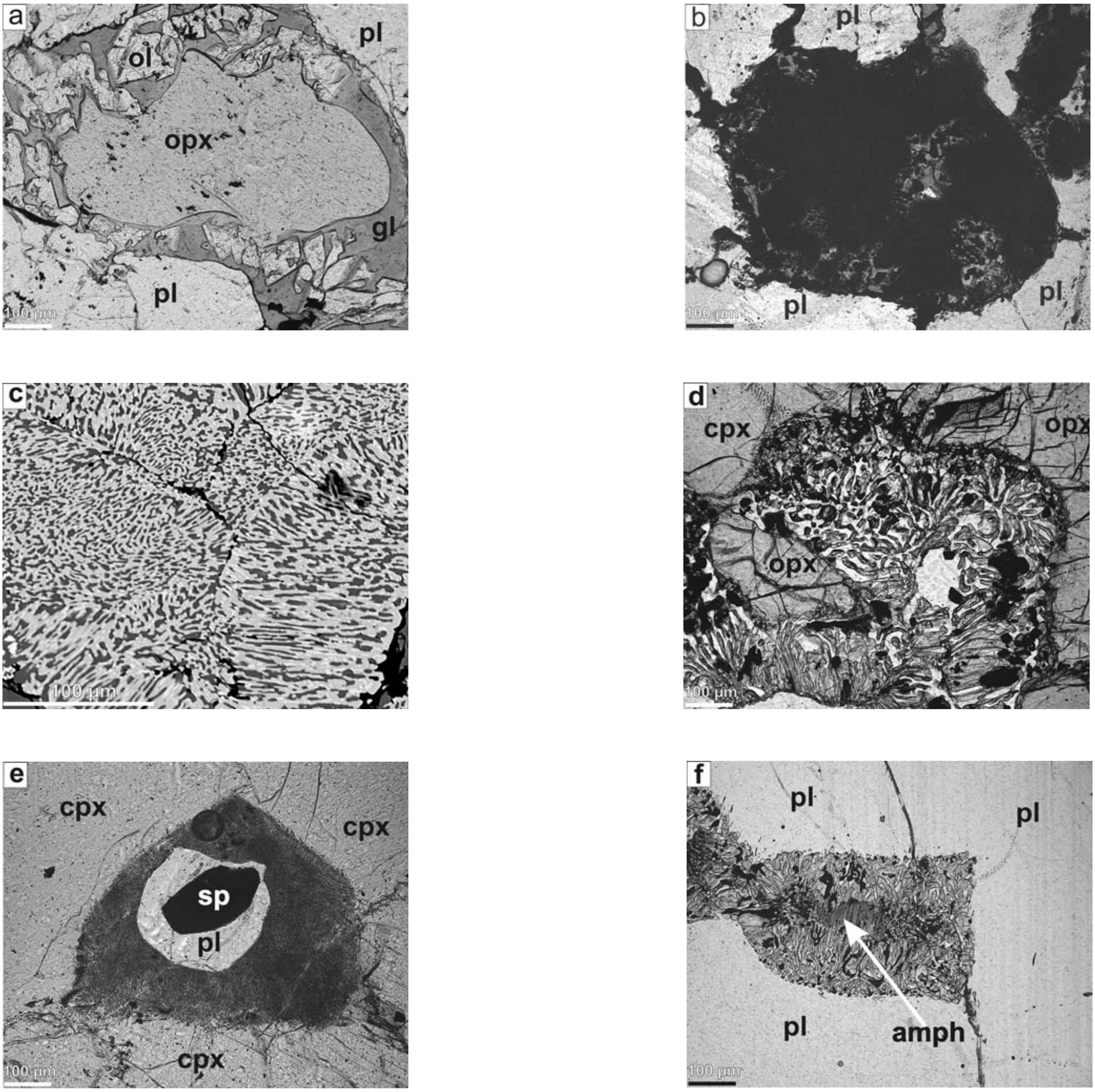

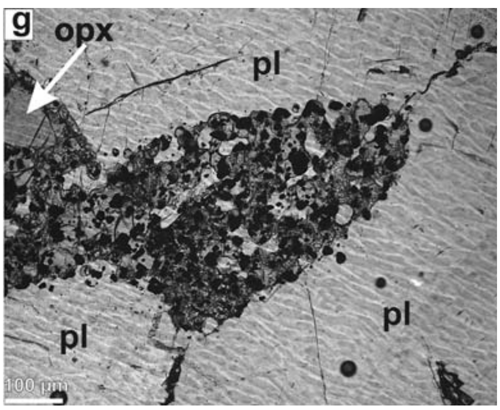

Fig. 1. A: Corona with glass and subhedral to skeletal olivine around primary orthopyroxene in the gabbronorite PBN 98-71. B: Fine-grained (type 1) plagioclase-orthopyroxene-spinel symplectite (ghost garnet) in PBN 98-75. C: Backscattered-electron image of the same symplectite (black, plagioclase; dark gray, orthopyroxene; light gray, spinel). D: Medium-grained (type 2) plagioclase-orthopyroxene-spinel symplectite in the gabbronorite PBN 98-73. E: Composite corona around spinel in the layered gabbronorite PBN 98-60. The first plagioclase rim is surrounded by type 1 plagioclase-orthopyroxene-spinel symplectite. F: Clinopyroxene-plagioclase-spinel symplectite (type 1) in the layered gabbronorite PBN 86-34. There is an amphibole relic in the core of the symplectite. G: Clinopyroxene-plagioclase-spinel symplectite (type 2) in the layered gabbronorite/pyroxenite PBN98-63.

electron-microprobe data on the main silicates and oxide phases) in order to constrain their magmatic origin and their metamorphic evolution. A few whole-rock REE analyses are also set out to discuss the nature of the protolith(s) of this suite of mafic xenoliths. Major and trace elements data on whole-rock samples will be presented in the forthcoming paper focusing on the magmatic differentiation of the ultramafic and mafic magmatic xenoliths.

Geological setting

The geological setting of the Beaunit Permian deep layered intrusion sampled by Late Cenozoic lavas has been discussed in detail by Féménias *et al.* (2003). A short summary is given below.

The Puy Beaunit Quaternary vent (dated at 43900 ± 5100 years; Rosseel, 1996) is one of the northernmost volcanoes of the Chaîne des Puys in the French Massif Central. This dual volcano is made of a maar (crosscut by the Ambène River) and three scoria cones (the Puys Gonnard) in the centre of the vent. All the xenoliths have been collected in the westernmost scoria cone.

Numerous mafic and ultramafic xenoliths with magmatic structures have been described; Féménias *et al.* (2003) suggest that they originated from a deep layered complex, emplaced during the Permian (257 ± 6 Ma, zircon U-Pb SIMS age), near the crust-mantle boundary. A transcurrent tectonic setting in the upper crust induced the local opening of pull-apart basins during Late Carboniferous and Permian (Arthaud & Matte, 1975; Mattauer & Matte, 1998). The crustal thinning associated with this opening led to an asthenospheric upwelling and partial melting of the uppermost mantle metasomatically enriched during a previous Devonian subduction event (Féménias *et al.*, 2003). The resulting calc-alkaline basaltic magmas were underplated at the crust-mantle boundary; this high temperature event probably led to minor granulitisation of the country rocks (Downes *et al.*, 1991; Féménias *et al.*, 2003).

Several similar Late Carboniferous and/or Permian magmatic complexes occur all across Europe; they are the evidence for the intense magmatic activity that occurred at Late Variscan times (see references in Féménias *et al.*, 2003).

Sample selection and analytical methods

Xenoliths (several cm to several dm in length) generally have polyhedral shapes. They are surrounded by a crust of basaltic host lava that consists of a black mesostasis with olivine, plagioclase, clinopyroxene and oxide phenocrysts. The infiltration of the lava in some xenoliths is evidenced by thin black veins.

This paper is only focused on mafic xenoliths because they have various and spectacular symplectitic and coronitic textures (see Fig. 1), thus giving the opportunity to constrain the P-T history of these samples from Permian to present day. Most mafic xenoliths are gabbronorites generally showing well-developed asymmetric layering. Some of them tend to disaggregate during sampling due to their poor cohesion; they were consolidated with epoxy resin for petrographic observation and electron-microprobe analysis.

Major-element composition of primary (millimetre-sized grains, *i.e.* magmatic or late magmatic sub-solidus phases) and secondary (*i.e.* phases in symplectitic intergrowths or in coronas around primary phases) phases has been analysed with a Camebax SX50 electron microprobe (CAMST, Université catholique of Louvain-la-Neuve, Belgium). The operating conditions involve an accelerating voltage of 15 kV, a beam current of 20 nA, an electron beam of 1 µm in diameter and a count time of 10-16 s per element. The bulk major-element composition of very fine-grained symplectites (grains < 5 µm) has also been obtained with a large defocused electron beam of 50 µm in diameter.

Rare earth element contents of the symplectites have been measured by LA-ICP-MS at the “Musée Royal de l’Afrique Centrale” (Tervuren, Belgium). The data were collected with a UV Fissons laser ablation microprobe coupled with a VG Elemental Plasma Quad (PQ2 Turbo Plus) ICP-MS. The craters are in the range of 40-60 µm in diameter. The calibration lines are based on the NIST 612 and NIST 610 synthetic standards and two laboratory mineral standards: a pyrope megacryst from the Shavaryn-Tsaram basalts (Mongolia) and a Cr-diopside from the Inagly dunite massif in Siberia. The data on each isotope peak were substracted from the blank and normalized to the ^{43}Ca signal (internal standard) and compared with the calibration lines. Accuracy of the analyses is in the range from 2 to 20 % (Féménias *et al.*, 2003) and dectection limits are in the range 10-20 ppb for La, Ce, Eu, Dy, Er and Yb and 30-50 ppb for Nd, Sm and Gd (Féménias *et al.*, 2003).

Whole-rock REE concentrations have been measured by ICP-MS at the “Collectif Interinstitutionnel de Géochimie Instrumentale” (University of Liège, Belgium). Analytical procedures and accuracy are described in Féménias *et al.* (2003).

Petrography

Mafic xenoliths are either homogeneous monolithologic or well-layered rocks. Lithology varies from leuco-gabbronorites (plagioclase-rich gabbronorites) to mela-gabbronorites (pyroxene-rich gabbronorites) with minor gabbros, norites and plagioclase-bearing pyroxenites. The modal proportions of the main phases, measured by image analysis of thin sections, are shown in Table 1. The layered samples show asymmetric anorthositic and pyroxenitic layers (see Fig. 4 in Féménias *et al.*, 2001) similar to those observed in typical stratiform intrusions such as the Bushveld and the Skaergaard complexes (Cawthorn, 1996). The layers are outlined by sharp contacts marked by the appearance or disappearance of a mineral phase (phase layering), but in a given layer, the modal proportions of cumulus phases vary gradually from bottom to top (modal layering).

Table 1. Modal proportions of the main phases in the Puy Beaunit mafic xenoliths.

Sample	Pl	Opx	Cpx	Grt[1]	Amph[2]	Oxide	Sum
PBN 86-34	80.4	0.6	0.6		18.5		100
PBN 98-60	28.8	28.2	25.4	6.6	-	11.0	100
PBN 98-62	50.1	10.2	20.8	-	12.5	6.4	100
PBN 98-63	39.2	9.7	30.6	-	16.5	4.0	100
PBN 98-73	43.4	32.9	11.5	11.7	-	0.5	100
PBN 98-75	58.8	-	-	32.9	-	8.3	100
PBN 98-76	55.2	20.3	9.0	-	-	15.6	100
PBN 98-77	23.6	11.9	55.6	<0.5	-	8.7	100
PBN 98-79	34.3	24.9	29.5	2.2	-	9.1	100
PBN 98-80	62.1	17.0	10.0	-	5.0	6.0	100
PBN 98-82	45.8	27.3	26.9	-	-	-	100
PBN 98-83	-	18.5	53.3	8.4	-	19.8	100
PBN 98-86	54.6	30.0	10.3	-	-	5.1	100
PBN 98-87	66.8	21.3	11.0	-	-	0.8	100
PBN 98-88	57.1	8.3	34.6	-	-	-	100
PBN 98-92	52.4	28.0	16.7	-	-	3.0	100
PBN 98-101	54.4	44.8	-	-	-	0.8	100
PBN 98-103	57.5	28.1	12.2	-	2.3	-	100
PBN 98-106	59.2	29.3	11.6	-	-	-	100
PBN 98-114	45.5	36.1	15.7	-	-	2.7	100

[1]Plagioclase-orthopyroxene-spinel symplectites
[2]Amphibole relics and clinopyroxene-plagioclase-spinel symplectites

Despite these classical cumulate structures, the rocks commonly show fine- to medium-grained polygonal texture partially blurred by the development of symplectitic and/or coronitic associations. The major mineral phases are plagioclase, ortho- and clinopyroxene, spinels, ilmenite and two ghost phases replaced by symplectitic associations (plagioclase-orthopyroxene-spinel and clinopyroxene-plagioclase-spinel symplectite respectively). Amphibole relics, apatite, zircon, rutile and srilankite are accessory. Orthopyroxene generally shows Schiller plates (plates of Fe-Ti oxides) along the cleavages, a feature considered as evidence for a magmatic origin (*i.e.* Ringuette *et al.*, 1999). No exsolutions were observed in clinopyroxene.

Most of the mafic xenoliths have well-developed coronas of brown-orange glass and skeletal to subhedral olivine around primary orthopyroxene (Fig. 1a) that clearly appears as anhedral relict grains. When such a corona is present, a brown glass is observed as interstitial material throughout the whole xenolith.

Xenoliths with plagioclase-orthopyroxene-spinel symplectites

Some gabbronorites and a plagioclase pyroxenite are characterised by the presence of plagioclase-orthopyroxene-spinel symplectites that mostly occur either as polygonal grains or more rarely in interstitial position. The polygonal morphology of the symplectite suggests that it completely replaces a (ghost) phase that was in textural equilibrium with the other primary phases. Modal proportions of this symplectite can be as high as 33 % (Table 1). Three different types of this symplectite have been recognized:

(1) Type 1 is composed of very thin (few micrometres) intergrowths of vermicular orthopyroxene and spinel (pleonaste) in plagioclase. These very fine-grained symplectites appear black under the polarizing microscope (Fig. 1b and c);

(2) Type 2 is composed of the same phases but it is coarser-grained (between 10 to 50 µm, Fig. 1d) than type 1. This symplectite locally constitutes the outer rim of type 1 symplectite;

(3) Type 3 consists of discrete spinel grains surrounded by a first rim of coarse plagioclase ± orthopyroxene and a second rim of type 1 symplectite (Fig. 1e).

These plagioclase-orthopyroxene-spinel intergrowths are actually comparable to those observed as kelyphites around garnet from garnet-bearing granulites, xenoliths in kimberlite and eclogites (Mitchell, 1986; Mukhopadhyay, 1991); they probably correspond to the destabilisation product of a former garnet.

Xenoliths with clinopyroxene-plagioclase-spinel symplectites

Some xenoliths (mainly gabbronorites, more rarely norites and plagioclase-bearing pyroxenites) contain symplectitic intergrowths (up to 19 %, Table 1) of plagioclase, clinopyroxene and titanomagnetite with minor pigeonite, orthopyroxene and glass. These intergrowths develop in euhedral to subhedral areas that could correspond to a primary ghost phase in textural equilibrium with other primary phases. Two types of symplectites have been distinguished:

(1) Type 1 consists of fine-grained (10-50 µm) intergrowths of vermicular plagioclase and Ti-magnetite in clinopyroxene, with minor orthopyroxene and pigeonite (Fig. 1f). An amphibole relic has been observed in the core of one of these symplectites in sample PBN 86-34;

(2) Type 2 is an optically continuous patchwork of clinopyroxene containing inclusions of subhedral plagioclase and Ti-magnetite with minor orthopyroxene, pigeonite and brown glass (Fig. 1g).

Mineral chemistry

Primary phases

The composition of primary plagioclase varies from An_{48} to An_{95} with the Or content ranging from Or_0 to Or_5 (Fig. 2a, Table 2). The xenoliths with polygonal texture and without any symplectitic intergrowth have primary labradorite (An_{48} to An_{72}, Fig. 2a) while the xenoliths with clinopyroxene-plagioclase-spinel symplectites and those with plagioclase-orthopyroxene-spinel symplectites have significantly more calcic plagioclases of bytownite composition, An_{62-87} and An_{82-94} respectively (Fig. 2a). The iron content of plagioclase is high, up to 0.65 wt% of FeO_{tot}. As no inclusions of Fe-Ti oxides were found, the iron is considered to be within the crystalline lattice of the feldspar.

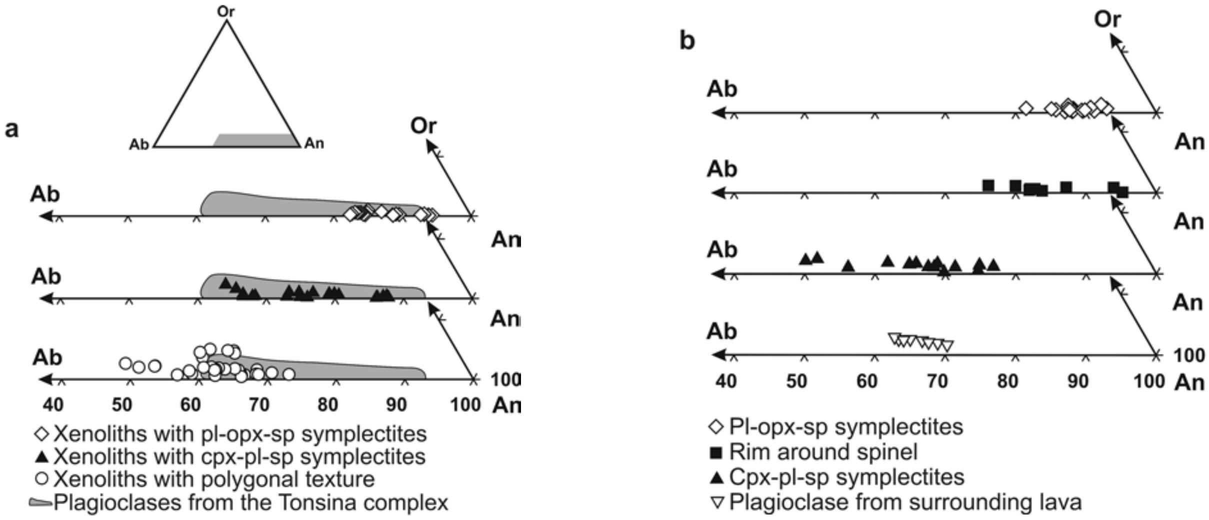

Fig. 2. Composition of the plagioclase. a) Primary plagioclase. b) Plagioclases in the different types of symplectite. Primary plagioclases are compared to those of the calc-alkaline Tonsina complex (DeBari & Coleman, 1989)

The Mg# of the primary orthopyroxenes and clinopyroxenes shows wide ranges of values from 80 to 52 and from 88 to 65 respectively (Fig. 3a, Table 3). The alumina content of these pyroxenes is high, up to 7.2 wt% of Al_2O_3.

The compositional variations of the primary silicate phases of the Beaunit mafic xenoliths are similar to those observed in the calc-alkaline Tonsina complex in Alaska (DeBari & Coleman, 1989). The trends of the Beaunit primary pyroxenes (Fig. 3a) also follow the sub-solidus trends defined by Skaergaard pyroxenes (Lindsley, 1983).

Primary oxides are mainly aluminous Ti-magnetites with minor ferri-pleonaste and ilmenite. Exsolutions of aluminous ulvöspinel and ilmenite (oxidized ulvöspinel) are locally present in aluminous Ti-magnetites.

The amphibole found as relict phase in the symplectites of PBN86-34 and as fresh grains in PBN86-28 is a Ti-pargasite (Mg#: 69-72; Table 4) following the nomenclature proposed by Leake *et al*. (1997).

Secondary phases

Coronas around orthopyroxene (glass and olivine)

The composition of the coronitic glass surrounding primary orthopyroxenes is intermediate between the compositions of the Quaternary basaltic glass from the host lava and of the primary orthopyroxene (Fig. 4, Table 5). The skeletal olivine in the glass has a composition ranging from Fo_{71} to Fo_{65}.

Plagioclase-orthopyroxene-spinel symplectites

The plagioclase in these symplectites is An-rich (from An_{81} to An_{93}, Fig. 2b, Table 2) with an Or content lower than Or_2. The plagioclase forming a rim around discrete spinel is also highly calcic (An_{95-75}). Secondary spinel is a ferri-pleonaste and the Mg# of secondary vermicular

Table 2. Selected representative analyses of primary and secondary plagioclases from the mafic xenoliths of Puy Beaunit.

Primary plagioclases							Secondary plagioclases					
wt%	PBN 98-73[a]	PBN 98-75[a]	PBN 98-63[b]	PBN 86-34[b]	PBN 98-82[c]	PBN 98-71[c]	PBN 98-60[a]	PBN 98-73[a]	PBN 98-60[a]	PBN 98-83[a]	PBN 98-114[b]	PBN 98-82[b]
SiO_2	44.24	47.43	46.28	51.67	49.70	54.45	44.63	45.46	44.35	45.70	49.32	56.10
Al_2O_3	34.27	32.32	33.33	29.29	31.02	28.17	34.15	33.01	34.43	33.67	31.03	26.58
FeO	0.59	0.45	0.33	0.45	0.26	0.41	0.89	1.14	0.75	1.57	0.74	0.69
MgO	0.04	0.12	0.03	0.12	0.05	0.06	0.10	0.08	0.09	0.41	0.10	0.17
CaO	19.24	16.97	17.66	13.60	15.10	10.87	19.05	18.15	19.22	17.02	15.53	10.24
Na_2O	0.70	1.62	1.59	3.90	3.04	5.20	0.76	1.31	0.64	1.40	2.90	5.63
K_2O	0.01	0.17	0.02	0.28	0.14	0.38	0.12	0.12	0.15	0.03	0.09	0.37
Total	99.07	99.07	99.23	99.32	99.31	99.54	99.69	99.28	99.63	99.80	99.70	99.77
Ab	6.14	14.57	13.96	33.62	26.51	45.38	6.72	11.45	5.65	12.89	25.11	48.82
An	93.79	84.42	85.94	64.78	72.68	52.43	92.61	87.84	93.49	86.93	74.37	49.08
Or	0.07	1.01	0.10	1.60	0.81	2.20	0.67	0.71	0.86	0.18	0.52	2.10

a: xenoliths with plagioclase-orthopyroxene-spinel symplectites. b: xenoliths with clinopyroxene-plagioclase-spinel symplectites.
c: xenoliths with polygonal texture.

Table 3. Selected representative analyses of primary and secondary pyroxenes.

wt%	PBN 98-114[a] cpx	PBN 98-80[a] cpx	PBN 98-106[a] cpx	PBN 86-28[a] opx	PBN 98-60[a] opx	PBN 98-106[a] opx	PBN 98-82[b] cpx	PBN 98-63[b] cpx	PBN 86-36[b] cpx	PBN 98-114[b] opx	PBN 98-82[b] opx	PBN 98-60[c] opx	PBN 98-73[c] opx
SiO_2	49.97	48.49	51.38	53.25	51.74	51.11	50.27	48.66	52.84	54.65	54.06	48.66	48.09
TiO_2	0.80	1.41	0.35	0.02	0.15	0.15	1.32	0.23	0.29	0.56	0.16	0.27	0.11
Al_2O_3	5.06	5.67	2.05	3.90	3.60	1.11	3.58	6.68	1.04	1.60	2.36	6.06	7.09
Cr_2O_3	0.35	0.12	0.00	0.20	0.02	0.01	0.54	0.11	0.00	0.06	0.05	0.03	0.03
FeO	6.82	9.46	11.54	13.31	20.05	27.82	7.34	10.16	15.02	11.39	15.68	22.74	20.47
MnO	0.14	0.09	0.35	0.34	0.14	0.53	0.18	0.33	0.46	0.31	0.29	0.41	0.82
MgO	13.64	11.75	12.29	27.58	23.50	17.58	15.34	13.25	18.80	29.25	26.68	19.34	20.60
CaO	22.34	21.75	21.48	1.04	0.47	0.66	20.66	19.53	11.30	1.74	0.77	1.59	1.57
Na_2O	0.71	0.84	0.36	0.08	0.00	0.02	0.36	0.73	0.21	0.04	0.05	0.05	0.04
Total	99.83	99.59	99.79	99.73	99.66	98.99	99.59	99.67	99.94	99.59	100.11	99.14	98.82
Mg#	86.55	76.88	67.98	79.74	68.37	52.98	84.22	79.87	70.57	82.57	75.25	61.92	67.31

a: primary pyroxenes.
b: pyroxenes in clinopyroxene-plagioclase-spinel symplectites.
c: pyroxenes in plagioclase-orthopyroxene-spinel symplectites.

orthopyroxene varies from 56 to 72 (Fig. 3b, Table 3). This orthopyroxene is quite Al- and Ca-rich (up to 8.5 wt% Al_2O_3 and 1.6 wt% CaO) presumably due to the composition of the primary ghost phase that has been replaced by the plagioclase-orthopyroxene-spinel symplectites (see below).

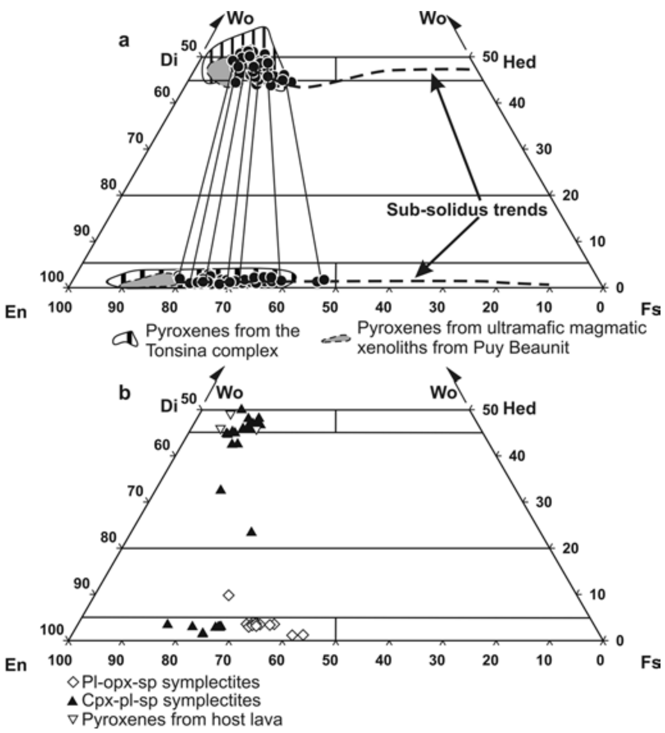

Fig. 3. Composition of primary pyroxenes (a) and of pyroxenes found in the different symplectites (b). Sub-solidus trends of Skaergaard pyroxenes from Lindsley (1983). Compositions of pyroxenes for ultramafic magmatic samples collected at Puy Beaunit are from Féménias *et al.* (2001) and the composition domain of magmatic clinopyroxenes of the Tonsina complex is from DeBari & Coleman (1989).

The major-element composition of the very fine-grained symplectites (Table 6) corresponds to a garnet of almandine-pyrope-grossular solid solution with a low spessartine content (< 2 mol%, Table 5). Similar garnets have been found in deep crustal mafic rocks and as phenocrysts in calc-alkaline volcanic rocks (Brousse *et al.*, 1972; Fitton, 1972; Mukhopadhyay, 1991; Day *et al.*, 1992; Harangi *et al.*, 2001, Fig. 5a).

Rare earth elements compositions of these symplectites have been measured by LA-ICP-MS (Table 7, Fig. 5b). The patterns show HREE enrichment with very low $(La/Yb)_N$ ratios (from 0.009 to 0.14). These patterns are similar to those of typical garnets which are characterised by a strong HREE enrichment (Hauri *et al.*, 1994).

Table 4. Selected representative analyses of amphiboles.

wt%	PBN 86-28 Fresh	PBN 86-28 Fresh	PBN 86-28 Relic	PBN 86-34 Relic	PBN 86-34 Relic
SiO_2	39.85	40.41	39.91	40.18	40.58
TiO_2	3.60	3.38	3.46	2.34	2.33
Al_2O_3	14.31	14.14	14.52	14.50	14.13
Cr_2O_3	0.47	0.32	0.50	0.07	0.13
FeO	9.92	9.50	9.68	11.17	11.87
MnO	0.12	0.08	0.07	0.10	0.12
MgO	13.63	13.94	13.80	13.78	13.86
CaO	10.93	10.97	11.11	11.03	10.98
Na_2O	2.50	2.45	2.53	2.38	2.29
K_2O	1.07	1.30	1.02	0.79	0.58
Total	96.40	96.47	96.60	96.34	96.86
Mg#	74.18	74.30	75.12	78.82	80.16

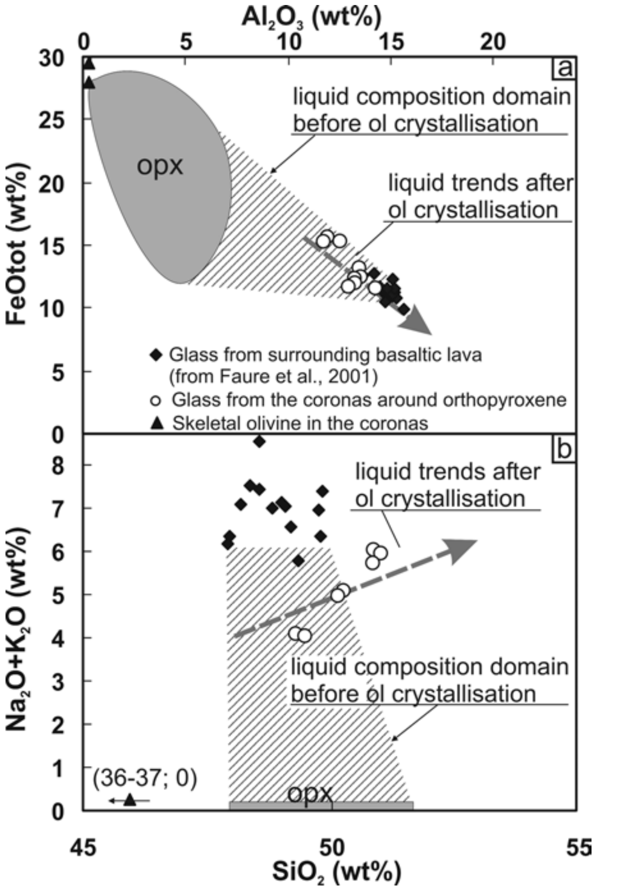

Fig. 4. FeO_{tot} *vs* Al_2O_3 (a) and total alkalis *vs* SiO_2 (TAS, b) diagrams illustrating the comparison between the glass of the coronas around primary orthopyroxene and the glass of the alkali basalt that encloses the xenoliths (Faure *et al.*, 2001). The grey domain represents the compositional field of the primary orthopyroxene.

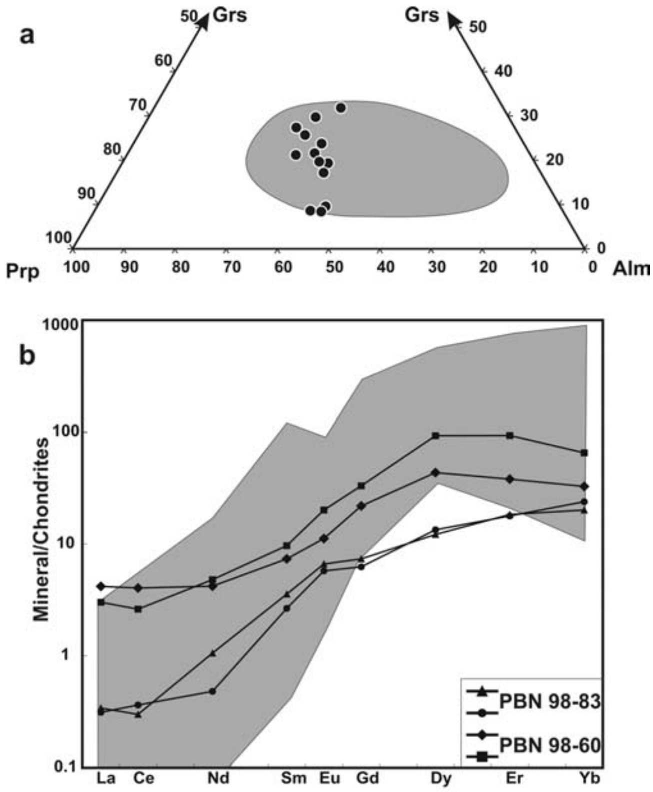

Fig. 5. Composition of plagioclase-orthopyroxene-spinel symplectites interpreted as ghost garnet in the Beaunit mafic xenoliths.
A: Composition in the system pyrope-grossular-almandine (mineral abbreviations after Kretz, 1983). The grey area indicates the compositional domain of garnet from calc-alkaline volcanic rocks and from experiments on the crystallisation of calc-alkaline liquids (Brousse *et al.*, 1972; Fitton, 1972; Day *et al*., 1992; Harangi *et al.*, 2001; Müntener *et al*., 2001; Aydar & Gourgaud, 2002).
B: REE patterns of the kelyphite compared to other garnet analysed by LA-ICP-MS. Data compiled from Mazzuchelli *et al.* (1992); Harangi *et al.* (2001) and Herman & Rubatto (2003).

Table 5. Composition of the glass and of the skeletal olivine in the coronas around primary orthopyroxene.

wt%	PBN 86-36 Glass	PBN 98-76 Glass	PBN 98-71 Glass	PBN 98-86 Olivine	PBN 98-63 Olivine
SiO_2	51.01	50.17	49.50	36.98	36.49
TiO_2	2.51	1.16	3.70	0.01	0.09
Al_2O_3	13.59	15.96	11.93	0.04	0.00
Cr_2O_3	0.02	0.02	0.00	0.03	0.06
FeO	12.40	15.72	15.61	27.25	30.15
MnO	0.21	0.42	0.19	0.46	0.59
MgO	3.57	3.59	4.35	34.39	32.22
CaO	8.08	5.03	7.94	0.33	0.37
Na_2O	3.28	2.30	2.75	0.02	0.01
K_2O	2.63	2.64	1.31	0.00	0.00
Total	97.30	97.02	97.28	99.50	99.97
Mg#	33.90	28.93	33.19		
Fo				69.23	65.58
Fa				30.77	34.42

Table 6. Bulk composition of plagioclase-orthopyroxene-spinel symplectites interpreted as former garnets.

wt%	PBN 98-75	PBN 98-75	PBN 98-60	PBN 98-60	PBN 98-60
SiO_2	39.73	38.86	39.28	39.67	39.60
TiO_2	0.10	0.05	0.20	0.13	0.07
Al_2O_3	22.61	22.90	22.67	22.17	22.22
Cr_2O_3	0.12	0.19	0.06	0.11	0.06
FeO	21.53	21.82	20.28	20.31	20.52
MnO	0.85	0.82	0.46	0.47	0.55
MgO	11.38	11.91	9.24	9.17	9.34
CaO	3.41	3.14	7.70	7.63	7.15
Na_2O	0.16	0.18	0.15	0.05	0.08
K_2O	0.01	0.01	0.04	0.00	0.00
Total	99.90	99.88	100.09	99.70	99.60
Alm	45.49	42.82	42.15	43.30	43.77
Grs	9.33	8.81	21.30	20.83	19.55
Prp	43.34	46.56	35.55	34.85	35.49
Sps	1.84	1.81	1.00	1.01	1.18

Table 7. REE composition of whole-rock samples by ICP-MS (a) and of fine-grained plagioclase-orthopyroxene-spinel symplectites (LA-ICP-MS), interpreted as former garnets (b).

a ppm	PBN 98-60	PBN 98-63	PBN 98-73	PBN 98-75	PBN 98-80	PBN 98-83	PBN 98-86	PBN 98-87	PBN 98-88	PBN 98-92	PBN 98-106
La	1.57	7.25	3.09	6.97	3.05	4.71	12.38	3.86	10.36	12.28	23.41
Ce	2.67	16.25	7.43	9.26	6.87	11.55	26.48	7.91	31.72	26.96	51.49
Pr	0.39	2.32	0.94	0.92	0.86	1.54	3.08	0.96	5.01	3.77	6.74
Nd	2.07	10.64	3.93	3.65	4.34	6.79	13.52	4.01	24.17	16.15	28.38
Sm	0.64	3.09	1.00	1.99	1.13	2.13	3.86	0.88	6.07	4.01	6.54
Eu	0.40	0.81	0.58	0.82	0.71	0.74	1.21	0.52	1.38	1.09	2.07
Gd	0.86	3.21	0.97	6.31	1.31	3.33	5.17	0.82	4.87	3.29	5.95
Tb	0.15	0.51	0.18	1.52	0.24	0.70	0.91	0.14	0.68	0.49	0.81
Dy	0.99	3.50	1.38	12.97	1.49	4.87	6.91	1.03	4.04	2.89	4.75
Ho	0.22	0.71	0.32	3.69	0.32	1.15	1.72	0.24	0.77	0.58	0.97
Er	0.63	2.22	1.00	11.54	0.95	2.98	4.75	0.73	2.15	1.68	2.55
Tm	0.09	0.35	0.17	1.84	0.16	0.40	0.66	0.12	0.32	0.24	0.39
Yb	0.60	2.22	1.07	12.69	0.89	2.39	4.36	0.72	1.80	1.54	2.43
Lu	0.07	0.31	0.15	2.01	0.12	0.30	0.64	0.09	0.25	0.18	0.36

b ppm	PBN 98-60	PBN 98-60	PBN 98-83	PBN 98-83
La	0.08	0.07	1.00	0.72
Ce	0.18	0.22	2.48	1.61
Nd	0.49	0.22	1.92	2.20
Sm	0.53	0.40	1.09	1.44
Eu	0.37	0.32	0.63	1.14
Gd	1.47	1.25	4.36	6.62
Dy	3.00	3.30	10.75	22.90
Er	2.95	2.86	6.11	14.98
Yb	3.25	3.86	5.29	10.54

Clinopyroxene-plagioclase-spinel symplectites

The plagioclase in these symplectites has an An content between An_{76} and An_{50} and an Or content between Or_1 and Or_2 (Fig. 2b, Table 2).

The secondary spinel is an aluminous Ti-magnetite. The Mg# of the secondary orthopyroxene ranges from 72 to 83 (Fig. 3b, Table 3); its titanium content is higher (from 0.4 to 0.6 wt% TiO_2) than those of other, primary and secondary, orthopyroxenes (< 0.3 wt% TiO_2).

Thermobarometric investigations

The mineral assemblages of the Beaunit mafic xenoliths can be used to estimate the P-T conditions that rocks experienced during their complex history, from their magmatic crystallisation and sub-solidus recrystallisation to their reequilibration when they were rising up to the surface.

The fine-grained plagioclase-orthopyroxene-spinel symplectites observed in many xenoliths are interpreted as resulting from the destabilisation of primary garnet. These symplectites generally have polygonal shape and display sharp contact with the primary silicate phases. This suggests that garnet was in chemical equilibrium with pyroxenes before its destabilisation and that pyroxene was clearly not involved during garnet breakdown. We thus feel that the bulk kelyphite composition is a reasonably good estimate of the garnet composition and that it can be used to infer P-T conditions from garnet-pyroxene pairs. Several authors (Mukhopadhyay, 1991; Stosch *et al.*, 1995; Embey-Isztin *et al.*, 2003) have demonstrated that the major-element composition of the fine-grained kelyphite partially replacing garnet is indeed very similar (less than 1 % difference of the relevant oxides; Mukhopadhyay, 1991) to that of preserved garnet. Moreover, the P-T conditions calculated from the kelyphite composition are not significantly different from those obtained with garnet composition (Stosch *et al.*, 1995 and Embey-Isztin *et al.*, 2003).

Amphibole barometers

Two geobarometers based on amphibole composition have been chosen to estimate the pressure of emplacement of deep-seated Puy Beaunit gabbroic rocks. Hollister *et al.* (1987) and Schmidt (1992) have calibrated barometers based on the aluminium content of hornblende in mafic plutonic rocks. These barometers are useful for amphiboles from calc-alkaline gabbros, even if a great uncertainty (± 0.2 GPa) is associated with the calculations.

These barometers have been applied to the cores of two relictual and three fresh amphiboles (22 analyses) from two mafic xenoliths of Beaunit. The two calibrations show similar results: the average pressure is 0.9 GPa (range: 0.85-0.97 GPa).

Garnet-orthopyroxene barometers

In mafic deep crustal rocks, the mutual solubility of aluminium between garnet and orthopyroxene is pressure dependent (Harley & Green, 1982; Harley 1984) and also depends on the Fe-Mg partitioning between the two phases. The uncertainties associated with these geobarometers are also quite high, around 0.2 GPa. As no relics of garnet have

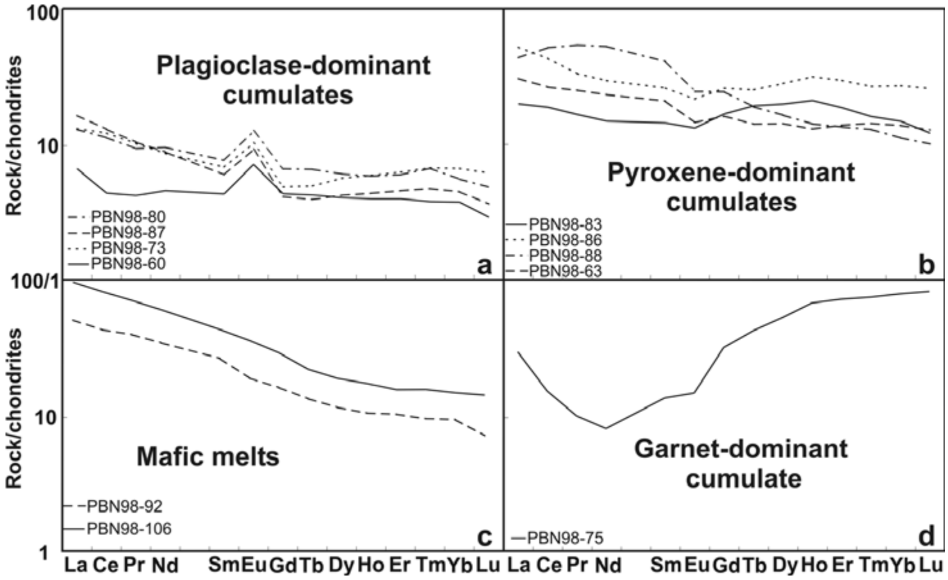

Fig. 6. Chondrite-normalised REE patterns for the different types of cumulate in Puy Beaunit mafic xenoliths. Normalising values are from McDonough & Sun (1995).

been found, the bulk composition of the very fine-grained plagioclase-orthopyroxene-spinel symplectites (type 1), interpreted as replacing garnet, has been used.

The calculation was made for 15 symplectite-orthopyroxene pairs with a temperature of 770°C (temperature given by the garnet-clinopyroxene pairs and by two-pyroxene thermometry, see below); it yields an average pressure of 1 GPa (0.92-1.03 GPa) with the calibration of Harley & Green (1982) and 1.1 GPa (0.97-1.15 GPa) with the calibration of Harley (1984).

Amphibole thermometer

The titanium content of amphibole varies linearly with the temperature for magmatic and recrystallised gabbros (Helz, 1973; Otten, 1984; Ernst & Liu, 1998). The thermometer of Otten (1984) has been calibrated for ilmenite-bearing gabbros equilibrated in the pressure range from 0.6 to 1 GPa. As the composition range and crystallisation conditions (*i.e.*, P, T, fO_2 and whole-rock H_2O content) of the gabbros studied by Otten (1984) are very similar to those of Beaunit mafic xenoliths, his calibration was used to estimate the crystallisation temperature of the brown amphibole in the Beaunit rocks. This temperature ranges from 930 to 1000°C, with an average of 970°C.

The thermometer proposed by Holland & Blundy (1994), based on amphibole-plagioclase equilibrium, has also been used for comparison purposes; it gives an average temperature of 950°C (range: 934-970°C). The uncertainty mentioned by the authors is about 40°C.

Garnet-clinopyroxene thermometer

The Fe-Mg partitioning between garnet and clinopyroxene is temperature dependent (Raheim & Green, 1974). Recently, Krogh Ravna (2000) proposed an updated calibration (with an uncertainty of ± 50°C) of this thermometer applicable to deep crustal mafic rocks. We used the fine-grained (type 1) plagioclase-orthopyroxene-spinel symplectites, isochemically replacing garnet, to estimate the temperature of formation. An average temperature of 770°C (range: 680-815°C) has been determined on 19 garnet-clinopyroxene pairs.

Two-pyroxene thermometry

The calibration of Bertrand & Mercier (1985) based on the Fe-Mg partitioning between coexisting ortho- and clino-pyroxene is appropriate for mafic rocks from the deep crust, average uncertainty being about 40°C. The temperature calculated using 75 primary pyroxene pairs for 18 rocks gives an average of 770°C (range: 668-843°C).

The temperatures calculated on 10 pairs of secondary pyroxenes in five clinopyroxene-plagioclase-spinel symplectites replacing amphiboles are significantly higher: 990°C (range: 869-1101°C).

Whole-rock REE geochemistry

The REE pattern of whole-rock mafic xenoliths can be used to infer the nature of the rocks (cumulates or liquids) as well as of the possible cumulus minerals. Several types of cumulate can be distinguished on the basis of the whole-rock REE patterns (Fig. 6, Table 6) and of the variations of the modal proportions of the main cumulus phases (plagioclase, pyroxene and garnet) even if the cumulus nature is difficult to assess in view of the sub-solidus recrystallisation of most xenoliths.

Plagioclase-dominant cumulates have been recognized: they are mainly leuco-gabbronorites and/or norites characterised by a LREE enrichment with $(La/Yb)_N$ varying from 1.8 to 3.7 and a strong positive Eu anomaly (Eu/Eu* from 1.7 to 1.8).

Pyroxene-dominant cumulates are mela-gabbronorites and plagioclase-bearing pyroxenites. They have slight negative Eu anomaly (Eu/Eu* = 0.8) with nearly flat and/or slightly LREE-enriched profiles ($(La/Yb)_N$ between 1.3 and 1.9). The LREE enrichment is probably due either to the presence of minor cumulus plagioclase or to trapped intercumulus liquid. One sample (PBN 98-83) shows a significant HREE enrichment (convex upward HREE pattern) probably due to the presence of minor cumulus garnet (replaced by kelyphite).

Mafic melts. Few gabbronorites are significantly more differentiated, they contain interstitial apatite and their whole-rock Mg# is rather low (down to 47). They are significantly enriched in REE (ΣREE up to 136 ppm), especially in LREE, with $(La/Yb)_N$ ratio between 5.4 and 6.5 and they don't show Eu anomaly. The fine-grained texture of these samples and the main geochemical characteristics show that these rocks are probably formed from liquids and are not cumulates.

Garnet-dominant cumulates. Sample PBN98-75 contains only plagioclase, ilmenite and very fine-grained symplectites with secondary plagioclase, orthopyroxene and spinel. These symplectites are interpreted as former garnets; the modal proportion of this "ghost garnet" is estimated at ~33 vol%. This rock has a peculiar REE pattern: it is REE-rich (ΣREE = 76.2 ppm) when compared to plagioclase and pyroxene cumulates (ΣREE < 54 ppm) and shows both LREE and HREE enrichment, with a relative depletion in intermediate REE, so that the $(La/Sm)_N$ ratio is greater than 1 (2.2) and the $(La/Yb)_N$ ratio is low (0.4). It also shows a negative Eu anomaly (Eu/Eu* = 0.6). This pattern could be due to the cumulation of both HREE-rich mineral such as garnet (Hauri *et al.*, 1994) and LREE-rich mineral (plagioclase).

Discussion

Origin of symplectites and coronas

The various symplectitic and coronitic textures can be interpreted as breakdown reactions of primary mineral phases of the mafic xenolith during a high-temperature, low-pressure metamorphic (solid state) event (see Vernon, 2004, for a recent review).

1) Plagioclase-orthopyroxene-spinel symplectites (including coronas developed around spinels)

These symplectites have bulk major element composition and the typical HREE enriched pattern of an almandine-pyrope garnet. The destabilisation of such garnet can be written as follows:

garnet → plagioclase + orthopyroxene + spinel (1).

This reaction is commonly observed in similar mafic and intermediate rocks (Mukhopadhyay, 1991; Thost *et al.*, 1991; Brodie, 1995; Zhao *et al.*, 2000; Jones & Escher, 2002; Elvevold *et al.*, 2003; Embey-Isztin *et al.*, 2003). Some authors (*e.g.* Mukhopadhyay, 1991) did propose another reaction:

garnet + clinopyroxene → plagioclase + orthopyroxene + spinel (2).

In our samples, clinopyroxenes do not appear involved in a reaction with garnet: indeed, the contact between the symplectites and the clinopyroxene is straight and sharp; moreover the rims of the clinopyroxene grain are compositionally identical to their core.

In details, however, the REE patterns of the symplectites are not strictly identical to those of garnets analysed by LA-ICP-MS (Mazzuchelli *et al.*, 1992; Harangi *et al.*, 2001; Hermann & Rubatto, 2003); the kelyphite from the mafic xenoliths of Beaunit have higher LREE. These slight differences could be explained by geological and/or analytical processes: (1) at the scale of mineral size, the kelyphite has probably a strongly heterogeneous REE distribution. LREE are probably concentrated in secondary plagioclase, while HREE are mainly in secondary pyroxene. During laser ablation of a small part (± 50 μm wide) of the symplectite, it is conceivable that one of these two phases has been oversampled; (2) Mukhopadhyay (1991) has shown that the garnet destabilisation is not strictly an isochemical process: the kelyphite is depleted in Mg and enriched in Ca and alkalis when compared to relictual garnet. It is also possible that some trace elements (like LREE) were mobilised during this destabilisation; (3) the REE composition of a garnet is generally positively correlated to the whole-rock REE content (Irving & Frey, 1978); (4) LREE are very low in garnet and are probably more sensitive to analytical errors.

2) Clinopyroxene-plagioclase-spinel symplectites

Amphibole relics have been found in the core zone of these secondary associations. Glass pockets found in the symplectites suggest that the first reaction was the melting of amphibole. This melt then started to crystallise, giving rise to the secondary association of clinopyroxene with inclusions of subhedral plagioclase and titanomagnetite. The precise mechanism of amphibole melting remains unknown; it could have been congruent or incongruent. Two sets of reaction can be written

- for congruent melting:

amphibole → $melt_1$ → clinopyroxene + plagioclase + Ti-magnetite ± orthopyroxene ± pigeonite ± $melt_2$ (3),

- for incongruent melting:

amphibole → clinopyroxene + $melt_1$

and

$melt_1$ → plagioclase + Ti-magnetite ± orthopyroxene ± pigeonite ± $melt_2$ (4).

Similar reactions have been described in mantle-derived ultramafic rocks (Varella *et al.*, 1999; Féménias *et al.*, 2001) and in andesitic rocks (*e.g.* Eggler 1972; Ruhterford & Hill, 1993; Devine *et al.*, 1998; Murphy *et al.*, 2000).

3) Coronas with glass and olivine.

We suggest that the infiltration of basaltic glass from the host lava inside some xenoliths has probably enhanced the partial melting of primary orthopyroxene. Indeed, the composition of glass around some orthopyroxenes is intermediate between the Quaternary basaltic glass and the primary orthopyroxene (Fig. 4). Subhedral to skeletal olivine started to crystallise from this mixed melt. The olivine crystallisation probably enriched the hybrid melt in SiO_2, Al_2O_3, Na_2O and K_2O as shown in Fig. 4. The reactions can be summarised as follows:

basaltic glass1 + opx $\rightarrow$ partially melted opx + glass2 (5).

glass2 $\rightarrow$ glass3 + olivine (6).

Faure *et al*. (2001) made detailed nano-petrographic investigations on these glass- and olivine-bearing coronas. They proposed similar but more complex mechanisms to explain their genesis: the reaction of the penetrating lava with the orthopyroxene has produced several generations of clinopyroxenes (cpx 1 to 5) and a small amount of melt.

Magmatic origin of the suite of mafic xenoliths

Asymmetric (mm- to cm- scale) layering observed in mafic xenoliths from Beaunit is a common feature of layered intrusions (Cawthorn, 1996). The parageneses of these mafic xenoliths are also typically magmatic; they are dominated by Ca-rich plagioclase, orthopyroxene, clinopyroxene, spinel, brown amphibole with accessory ilmenite, apatite and zircon. Only garnet is generally considered to be of metamorphic origin (this issue is discussed below). The presence of numerous Schiller plates in orthopyroxene is also cited as evidence for the magmatic origin of the pyroxene (Ringuette *et al*., 1999). The mafic xenoliths from Beaunit probably derived from one (or several) deep layered intrusion(s) located in the deep crust or near the crust-mantle boundary (Féménias *et al*., 2001, 2003). Moreover, Féménias *et al*. (2001) have shown that some layered samples display both mafic and ultramafic thin layers suggesting the cogenetic character of ultramafic and mafic magmatic samples.

Even if these samples underwent sub-solidus re-equilibration under granulite-facies conditions, as attested by the general polygonal texture of most mafic samples, this does not correspond, strictly speaking, to a "metamorphic event" but rather to an isobaric cooling, common in similar deep-seated intrusions (DeBari & Coleman, 1989; Cawthorn, 1996). Moreover, there is no new metamorphic mineral formed during this sub-solidus re-equilibration. It is thus ambiguous to name these rocks "granulites" even if the composition of the mineral phases was modified during the re-equilibration process under granulites facies conditions. This kind of re-equilibration does not totally erase the magmatic composition of the minerals and thus parameters such as Mg% of pyroxenes or An% of plagioclase can still be used to decipher magmatic differentiation processes (DeBari & Coleman, 1989; Cawthorn, 1996).

Mafic xenoliths from Puy Beaunit are mainly cumulate gabbronorites that were affected by a low-P, high-T recrystallisation event under static conditions, as attested by the presence of numerous coronas and symplectites around primary phases. We rather refer to these rocks as meta-cumulates or meta-gabbronorites rather than granulites. Moreover, Leyreloup (1974) already made the distinction (for French Massif Central xenoliths) between "real granulites" (*i.e.* basic charnockites) and what he named "semelle gabbro-norito-péridotitique" made of magmatic coronitic gabbros, pyroxenites and peridotites. Mafic xenoliths from Puy Beaunit belong to this last suite and are clearly distinct from the granulites suite as described by Leyreloup (1974).

The calc-alkaline Tonsina complex (DeBari & Coleman, 1989) shows numerous similarities with mafic xenoliths from Puy Beaunit: (1) associations between mafic and ultramafic cumulates (harzburgites, dunites, websterites; Féménias *et al*., 2001); (2) presence of garnet- and amphibole-bearing gabbros and gabbronorites; (3) high proportions (up to 20 %) of magmatic amphibole; (4) presence of highly calcic plagioclase as late cumulate phase (crystallising after olivine, pyroxenes and spinel); (5) high pressure of emplacement and crystallisation (~ 1 GPa). Féménias *et al*. (2003) have already demonstrated that magmatic ultramafic samples that are sometimes interlayered with the mafic samples have a calc-alkaline geochemical affinity. The mafic xenoliths described in this paper are thus presumably also of calc-alkaline affinity, but this has to be confirmed by whole-rock major and trace elements compositions (work in progress).

Preliminary REE geochemical data suggest that pyroxenes, plagioclase and garnet were cumulus phases. Garnet does not result from metamorphic reaction between pyroxenes and plagioclase during metamorphism under granulite-facies conditions. It directly crystallised from the magma that gave rise to the various ultramafic and mafic rocks collected at Beaunit.

It can indeed be demonstrated that garnet is obviously not inherited from the surrounding metapelitic granulites because:

(1) infusible garnet from surrounding meta-pelites would probably have reacted with the mafic magma, it would show anhedral, relict morphology. This is not the case; the "ghost garnet", completely replaced by the fine-grained orthopyroxene-plagioclase-spinel symplectites, is polygonal and was in textural equilibrium with the other primary phases as shown above;

(2) metasedimentary garnets from granulites generally have higher Mn (> 4 mol% of spessartine) and lower Ca contents than the magmatic garnets (Harangi *et al*., 2001; Jung & Mezger, 2003; Embey-Isztin *et al*., 2003);

(3) the ghost garnet is not present in all lithologies. For example, it is absent in a thin anorthositic layer of a composite xenolith (PBN98-60) although it was observed in the gabbronoritic layers of this xenolith. It is also totally absent in ultramafic samples (Féménias *et al*., 2001).

Fractionation of almandine-pyrope garnet from basaltic to rhyolitic calk-alkaline liquids at high pressure (about 1 GPa) has been observed in natural systems (Brousse *et al*., 1972; Fitton, 1972; Barley, 1987; DeBari & Coleman, 1989; Day *et al*., 1992; Ringuette *et al*., 1999; Harangi *et al*., 2001; Aydar & Gourgaud, 2002) and in experiments (Green & Ringwood, 1968a & b; Green, 1982; Müntener *et al*., 2001; Ulmer *et al*., 2003). Such garnet could also be the result from late-magmatic sub-solidus re-equilibration of the intrusion during isobaric cooling (DeBari & Coleman, 1989). This may explain the interstitial position of the garnet in some samples.

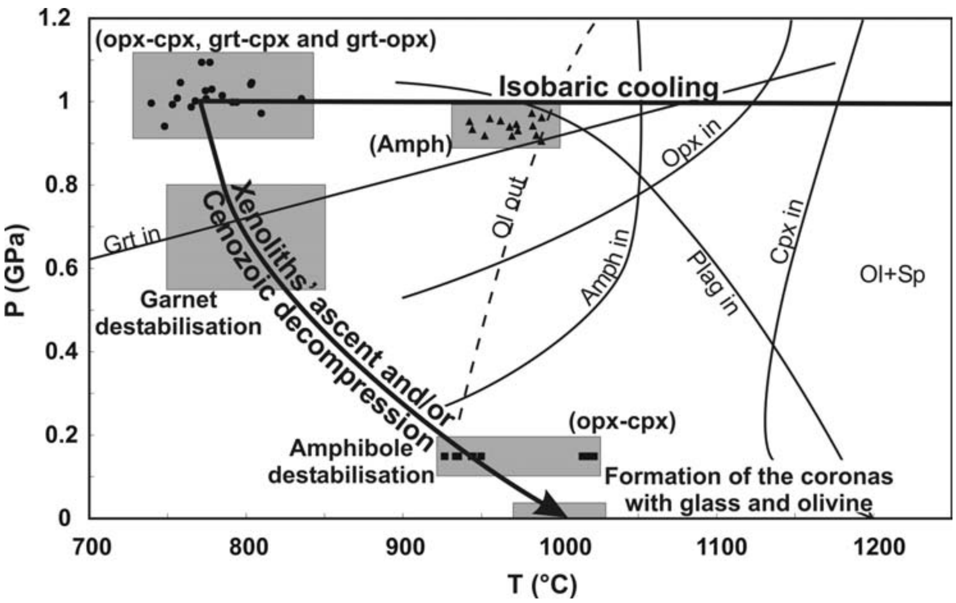

Fig. 7. P-T history recorded by the mafic xenoliths of Puy Beaunit superimposed on the phase diagram of basalt crystallisation (from Nimis & Ulmer, 1998). Grt-in curve is from Green (1967). Pressure of destabilisation of amphibole (0.15 GPa) is from Devine *et al.* (1998). Mineral pairs used to estimate the P-T conditions are indicated between brackets.

It appears from the above considerations that the "ghost garnet" of the mafic xenoliths of Beaunit is probably of magmatic origin and not metamorphic nor inherited. This magmatic garnet can be used to constrain the composition of the source material and of the parental magmatic liquid as well, because it is rather uncommon in mafic cumulates. Harangi *et al*. (2001) argue that magmatic almandine garnet in basic to intermediate rocks is characteristic of calc-alkaline magmas generated by partial melting of hydrated mantle source. The liquid crystallising the gabbros could be a hydrated, high-alumina basalt, crystallising under pressures comprised between 0.7 and 1.2 GPa (DeBari & Coleman, 1989; Harangi *et al*., 2001; Ulmer *et al*., 2003).

Crystallisation, sub-solidus re-equilibration and destabilisation: a P-T-t record

The P-T conditions (900-1000°C and 0.9-1.1 GPa) inferred from the composition of amphibole probably correspond to the crystallisation of the Beaunit cumulates. These conditions agree reasonably well with those inferred from the phase diagram of Nimis & Ulmer (1998). The presence of magmatic garnet is also an indication of the high pressure of crystallisation, in the range 0.7-1.1 GPa (Green & Ringwood 1968a; Ulmer *et al*., 2003; Harangi *et al*., 2001).

The mafic rocks were re-equilibrated during the isobaric cooling of the intrusion, as evidenced by the polygonal texture of most xenoliths. The P-T conditions prevailing during this re-equilibration were estimated from the garnet-clinopyroxene and orthopyroxene-clinopyroxene pairs (T) and from the orthopyroxene-garnet pair (P); they are in the range 770 ± 50°C and 0.9-1.1 GPa.

The fine-grained plagioclase-orthopyroxene-spinel symplectites are interpreted as the nearly isochemical breakdown of garnet during decompression. This process is thought to occur at about 750-850°C and 0.55-0.8 GPa according to Brodie (1995), Zhao *et al*. (2000) and Elvevold *et al*. (2003). These conditions are in agreement with the experimental data of Green (1967) as shown in Fig. 7.

This pressure decrease can not be related to a late-Variscan metamorphic event because the emplacement and crystallisation of the Beaunit deep layered intrusion occurred during Permian and is one of the latest tectono-metamorphic of the late-Variscan period in French Massif Central (Féménias *et al*., 2003). The lower crust below Beaunit has thus probably been stable from Late-Permian to Cenozoic, *i.e.* when the Limagne Graben formed. Two mechanisms can explain this low-P event: (1) lower crust uplift induced by Cenozoic extensional tectonic and (2) transport of the xenoliths to the surface by the Quaternary host lava.

Long-lived decompression in extensional setting would probably have modified the composition of rim (and maybe also of the core) of the pyroxenes (decrease of Al content), as shown in the xenoliths collected in Sierra-Nevada (Mukhopadhyay, 1991). In the mafic xenoliths from Beaunit, the thermobarometry applied to the main silicate phases does not show any evidence of re-equilibration under 0.55-0.8 GPa, where garnet is no more stable.

In the Beaunit samples, garnet has been totally replaced by symplectitic association. As the ascent of the lava has been very rapid (about 16 hours according to Faure *et al.*, 2001) the xenoliths taken up by the lava underwent a very quick decompression, which is unlikely to allow complete garnet breakdown. Such a rapid process would have produced only thin kelyphitic rims around preserved garnet (Misra *et al.*, 2004). Whatever the exact mechanism responsible for the destabilisation of garnet, the two suggested processes were simultaneous and may be combined.

The breakdown of amphibole occurs at high temperature (950-1050°C) as indicated by the two-pyroxene thermometry on symplectitic secondary assemblages and probably at shallow level during xenolith ascent, below 0.15 GPa for Devine *et al*. (1998) and below 0.3 GPa following the phase diagram of Nimis & Ulmer (1998).

Temperature and pressure during the formation of coronas with glass and olivine around orthopyroxene have been estimated by Faure *et al*. (2001): they are at about 1000°C and at very low P. These coronas were probably induced by the penetration of a small amount of host lava inside the xenoliths.

Conclusions

• Mafic xenoliths from Puy Beaunit are essentially gabbronorites and gabbros, some of them displaying layered textures. They crystallised at pressures close to 0.9-1.0 GPa at about 1000°C. They were re-equilibrated under sub-solidus conditions at 770°C and ~ 1 GPa during the isobaric cooling of the intrusion.

• Primary garnet has been totally transformed to a fine-grained plagioclase-orthopyroxene-spinel symplectite, during lower-crust uplift induced by Cenozoic extensional tectonic and/or during the first step of xenolith ascent in the Quaternary Beaunit alkali basalt. Magmatic amphibole (Ti-pargasite) melted in response to the brutal increase of temperature due to the xenolith uptake in the host lava. This melt crystallised the clinopyroxene-plagioclase-spinel intergrowths observed in many samples. Orthopyroxene, surrounded by a corona with glass and olivine, also began to melt due to a reaction with small amounts of infiltrating host volcanic glass.

• Most xenoliths are cumulates of a mafic hydrated calc-alkaline magma. The main cumulus phases are: plagioclase, pyroxene and garnet. A few basic melts have also been identified. The garnet is most presumably of magmatic origin, similar garnets are known in calc-alkaline lavas and in deep roots of volcanic arc (*i.e.* Tonsina Complex in Alaska).

Acknowledgements : The detailed and constructive reviews of M. Grégoire, J. Hermann and C. Chopin are gratefully acknowledged. José Berger is also warmly acknowledged for his helpful corrections for the English. Special thanks are due to Giovanni Bernardinis for the preparation of the delicate thin sections of the Beaunit mafic xenoliths.

References

Arthaud, F. & Matte, P. (1975): Les décrochements tardi-hercyniens du sud-ouest de la France. Géométrie et essai de reconstitution des conditions de la déformation. *Tectonophysics*, **25**, 139-171.

Aydar, E. & Gourgaud, A. (2002): Garnet-bearing basalts: an example from Mt Hasan, Central Anatolia, Turkey. *Mineral. Petrol.*, **75**, 185-201.

Barley, M.E. (1987): Origin and evolution of mid-Cretaceous, garnet-bearing, intermediate and silicic volcanics from Canterbury, New Zealand. *J. Volcanol. Geotherm. Res.*, **32**, 247-267.

Berger, E. & Forette, M.C. (1975): Réactions de basaltes alcalins des Causses, du Vivarais et du Velay (France) avec les xénocristaux des enclaves homéogènes. *Bull. Soc. fr. Minéral. Cristallogr.*, **98**, 366-373.

Bertrand, P. & Mercier, J.C.C. (1985): The mutual solubility of coexisting ortho- and clinopyroxene: toward an absolute geothermometer for the natural systems? *Earth. Planet. Sci. Lett.*, **76**, 109-122.

Braun, I. & Kriegsman, L.M. (2001): Partial melting in crustal xenoliths and anatectic migmatites: a comparison. *Phys. Chem. Earth.*, **26**, 261-266.

Brodie, K.H. (1995): The development of orientated symplectites during deformation. *J. metamorphic Geol.*, **13**, 499-508.

Brousse, R., Bizouard, H., Salat, J. (1972): Grenats des andésites et des rhyolites de Slovaquie, origine des grenats dans les séries andésitiques. *Contrib. Mineral. Petrol.*, **35**, 201-213.

Cawthorn, R.G. (ed.) (1996): Layered intrusions. Elsevier Science B.V., Amsterdam, 531p.

Day, R.A., Green, T.H., Smith, I.E.M. (1992): The origin and significance of garnet phenocrysts and garnet-bearing xenoliths in Miocene calc-alkaline volcanics from Northland, New Zealand. *J. Petrol.*, **33**, 125-161.

DeBari, S.M. & Coleman, R.G. (1989): Examination of the deep levels of an island arc: evidence from the Tonsina ultramafic-mafic assemblage, Tonsina, Alaska. *J. Geophys. Res.*, **94**, 4373-4391.

Devine, J.D., Gardner, J., Rutherford, M.J. (1998): Petrologic determination of magma ascent rates for the 1995-1997 Soufriere Hills volcano andesitic magma. *Geophys. Res. Lett.*, **25**, 3673-3676.

Downes, H., Kempton, P.D., Briot, D., Harmon, R.S., Leyreloup, A.F. (1991): Pb and O isotope systematics in granulites facies xenoliths, French Massif Central: implication for crustal processes. *Earth. Planet. Sci. Lett.*, **102**, 342-357.

Eggler, D.H. (1972): Amphibole stability in H_2O-undersatured calc-alkaline melts. *Earth. Planet. Sci. Lett.*, **115**, 28-34.

Elvevold, S., Thrane, K., Gilotti, J.A. (2003): Metamorphic history of high pressure granulites in Payer Land, Greenland Caledonides. *J. metamorphic Geol*., **21**, 49-63.

Embey-Istzin, A., Downes, H., Kempton, P.D., Dobosi, G., Thirwall, M. (2003): Lower crustal granulite xenoliths from the Pannonian Basin, Hungary. Part 1: Mineral chemistry, thermobarometry and petrology. *Contrib. Mineral. Petrol*., **144**, 652-670.

Ernst, W.G. & Liu, J. (1998): Experimental phase-equilibrium study of Al- and Ti-contents of calcic amphibole in MORB-A semi-quantitative thermobarometer. *Am. Mineral.*, **83**, 952-969.

Faure, F., Trolliard, G., Montel, J.M., Nicollet, C. (2001): Nanopetrographic investigation of a mafic xenolith (maar de Beaunit, Massif Central, France). *Eur. J. Mineral.*, **13**, 27-40.

Féménias, O., Mercier, J.C.C., Demaiffe, D. (2001): Pétrologie des xénolites ultramafiques du puy Beaunit (Massif central français): un gisement atypique du manteau sous-continental. *C. R. Acad. Sci. Paris.*, **332**, 535-542.

Féménias, O., Coussaert, N., Bingen, B., Whitehouse, M., Mercier, J.C.C., Demaiffe, D. (2003): A Permian underplating event in late- to post-orogenic tectonic setting. Evidence from the mafic-ultramafic layered xenoliths from Beaunit (French Massif Central). *Chemical Geol.*, **199**, 293-315.

Fitton, J.G. (1972): The genetic significance of almandine-pyrope phenocrysts in the calc-alkaline Borrowdale volcanic group, Northern England. *Contrib. Mineral. Petrol.*, **36**, 231-248.

Green, T.H. (1967): An experimental investigation of the subsolidus assemblages formed at high pressure in high alumina basalt, kyanite eclogite and grosspydite composition. *Contrib. Mineral. Petrol.*, **16**, 84-114.

Green, T.H. & Ringwood, A.E. (1968a): Genesis of the calc-alkaline igneous rock suite. *Contrib. Mineral. Petrol.*, **18**, 105-162.

— (1968b): Origin of garnet phenocrysts in calc-alkaline rocks. *Contrib. Mineral. Petrol.*, **18**, 163-174.

Green, T.H. (1982): Anatexis of mafic crust and high pressure crystallisation of andesite. *In* "Andesites: orogenic andesites and related rocks". R.S. Thorpe, ed. Chichester, Wiley, 465-487.

Harangi, S.Z., Downes, H., Kósa, L., Szabó, C.S., Thirlwall, M.F., Mason, P.R.D., Mattey, D. (2001): Almandine garnet in calc-alkaline volcanic rocks of the northern Pannonian basin (Eastern-Central Europe): geochemistry, petrogenesis and geodynamic implications. *J. Petrol.*, **42**, 1813-1843.

Harley, S.L. (1984): The solubility of alumina in orthopyroxene coexisting with garnet in FeO-MgO-Al_2O_3-SiO_2 and CaO-FeO-MgO-Al_2O_3-SiO_2. *J. Petrol.*, **25**, 665-696.

Harley, S.L. & Green, D.H. (1982): Garnet-orthopyroxene barometry for granulites and peridotites. *Nature*, **300**, 697-702.

Hauri, E.H., Wagner, T.P., Grove, T.L. (1994): Experimental and natural partitioning of Th, U, Pb and other trace elements between garnet, clinopyroxene and basaltic melts. *Chemical Geol.*, **117**, 149-166.

Helz, R.T. (1973): Phase relation in basalts in their melting range at P_{H2O}= 5 kbar as a function of oxygen fugacity. Part I. Mafic phases. *J. Petrol.*, **14**, 249-302.

Hermann, J. & Rubatto, D. (2003): Relating zircon and monazite domains to garnet growth zones: age and duration of granulite facies metamorphism in the Val Malenco lower crust. *J. metamorphic Geol.*, **21**, 833-852.

Hermann, J., Müntener, O., Trommsdorff, V., Hansmann, W., Piccardo, G.B. (1997): Fossil crust-to-mantle transition, Val Malenco (Italian Alps). *J. Geophys. Res.*, **102**, 20123-20132.

Holland, T. & Blundy, J. (1994): Non ideal interactions in calcic amphiboles and their bearing on amphibole-plagioclase thermometry. *Contrib. Mineral. Petrol.*, **116**, 433-447.

Hollister, L.S., Grissom, G.C., Peters, E.K., Stowell, H.H., Sisson, V.B. (1987): Confirmation of the empirical correlation of Al in hornblende with pressure of solidification of calc-alkaline plutons. *Am. Mineral.*, **72**, 231-239.

Irving, A.J. & Frey, F.A. (1978): Distribution of trace-elements between garnet megacryst and host volcanic liquid of kimberlitic to rhyolitic composition. *Geochim. Cosmochim. Acta*, **42**, 771-781.

Jones, K.A. & Escher, J.C. (2002): Near-isothermal decompression within a clockwise P-T evolution recorded in migmatitic mafic granulites from Clavering Ø, NE Greenland: implications for the evolution of the Caledonides. *J. metamorphic Geol.*, **20**, 365-378.

Jung, S. & Mezger, K. (2003): Petrology of basement-dominated terranes: I. Regional metamorphic T–t path from U–Pb monazite and Sm–Nd garnet geochronology (Central Damara orogen, Namibia). *Chemical Geol.*, **198**, 223-247.

Kretz, R. (1983): Symbols for rock-forming minerals. *Am. Mineral.*, **68**, 277-279.

Krogh Ravna, E. (2000): The garnet-clinopyroxene Fe2+-Mg geothermometer: an updated calibration. *J. metamorphic Geol.*, **18**, 211-219.

Leake, B. E., Woolley, A. R., Arps, C. E. S., Birch, W. D., Gilbert, M. C., Grice, J.D., Hawthorne, F.C., Kato, A., Kisch, H.J., Krivovichev, V.G., Linthout, K., Laird, J., Mandarino J., Maresch, W.V., Nickel, E.H., Rock, N.M.S., Schumacher, J.C., Smith, D.C., Stephenson, N.C.N., Ungaretti, L., Whittaker, E.J.W., Youzhi, G. (1997): Nomenclature of amphiboles: Report of the Subcommittee on Amphiboles of the International Mineralogical Association Commission on new minerals and mineral names. *Eur. J. Mineral.*, **9**, 623-652.

Leyreloup, A.F. (1974): Les enclaves catazonales remontées par les éruptions néogènes de France: nature de la croûte inférieure. I. Lithologie et structurologie d'ensemble du complexe granulito-charnockitique sous-jacent au Massif Central français d'après les enclaves remontées par les volcans néogènes. *Contrib. Mineral. Petrol.*, **46**, 17-27.

Lindsley, D.H. (1983): Pyroxene thermometry. *Am. Mineral.*, **68**, 477-493.

Mattauer, M. & Matte, P. (1998): Le bassin stéphanien de St-Etienne ne résulte pas d'une extension généralisée: c'est un bassin pull-apart en relation avec un décrochement dextre. *Geodyn. Acta*, **11**, 23-31.

Mazzucchelli, M., Rivalenti, G., Vannucci, R., Bottazzi, P., Ottolini, L., Hofmann, A.W., Sinigoi, S., Demarchi, G. (1992): Trace element distribution between clinopyroxene and garnet in gabbroic rocks of deep crust: An ion microprobe study. *Geochim. Cosmochim. Acta*, **56**, 2371-2385.

McDonough, W.F. & Sun, S.S. (1995): The composition of the earth. *Chemical Geol.*, **120**, 223-253.

Misra, K.C., Anand, M., Taylor, L.A., Sobolev N.V. (2004): Multi-stage metasomatism of diamondiferous eclogite xenoliths from the Udachnaya kimberlite pipe, Yakutia, Siberia. *Contrib. Mineral. Petrol.*, **146**, 696-714.

Mitchell, R.H. (1986): Kimberlites. Mineralogy, Geochemistry and Petrology. Plenum Press, New York, 442 p.

Mukhopadhyay, B. (1991): Garnet breakdown in some deep-seated garnetiferous xenoliths from the central Sierra Nevada: Petrologic and tectonic implications. *Lithos*, **27**, 59-78.

Müntener, O., Kelemen, P.B., Grove, T.L. (2001): The role of H_2O during crystallisation of primitive arc magmas under uppermost mantle conditions and genesis of igneous pyroxenites: an experimental study. *Contrib. Mineral. Petrol.*, **141**, 643-658.

Murphy, M.D., Sparks, R.S.J., Barclay, J., Carroll, M.R., Brewer, T.S. (2000): Remobilization of andesite magma by intrusion of mafic magma at the Soufriere Hills volcano, Montserrat, West Indies. *J. Petrol.*, **41**, 21-42.

Nimis, P. & Ulmer, P. (1998): Clinopyroxene geobarometry of magmatic rocks: part I. An expanded structural geobarometer for anhydrous and hydrous, basic and ultrabasic systems. *Contrib. Mineral. Petrol.*, **133**, 122-135.

Otten, M.T. (1984): The origin of brown hornblende in the Artfjallet gabbro and dolerites. *Contrib. Mineral. Petrol.*, **86**, 189-199.

Raheim, A. & Green, D.H. (1974): Experimental determination of the temperature and the pressure dependence of the Fe-Mg partition coefficient for garnet and clinopyroxene. *Contrib. Mineral. Petrol.*, **48**, 179-203.

Ringuette, L., Martignole, J., Windley, B.F. (1999): Magmatic crystallization, isobaric cooling and decompression of the garnet-bearing assemblages of the Jijal sequence (Kohistan terrane, western Himalayas). *Geology*, **27**, 139-142.

Rosseel, J.B. (1996): Synthèse chrono-magmatologique de la Chaîne des Puys. Unpublished diploma thesis (DEA), Univ. B. Pascal, Clermont Ferrand II, 50 p.

Rutherford, M.J. & Hill, P.M. (1993): Magma ascent rates from amphibole breakdown: an experimental study applied to the 1980-1986 Mount St-Helens eruptions. *J. Geophys. Res.*, **98**, 19667-19685.

Schmidt, M.W. (1992): Amphibole composition as a function of pressure: an experimental calibration of the Al-in-hornblende thermometer. *Contrib. Mineral. Petrol.*, **110**, 304-310.

Stosch, H.G., Ionov, D.A., Puchtel, I.S., Galer, S.J.G., Sharpouri, A. (1995): Lower crustal xenoliths from Mongolia and their bearing on the nature of the deep crust beneath central Asia. *Lithos*, **36**, 227-242.

Thost D.E., Hensen B.J., Motoyoshi Y. (1991): Two-stage decompression in garnet-bearing mafic granulites from Sostrene Island, Prydz Bay, East Antarctica. *J. metamorphic Geol.*, **8**, 245-266.

Ulmer, P., Müntener, O., Alonso Perez, R. (2003): Potential role of garnet fractionation in H_2O-undersaturated andesite liquids at high pressure: An experimental study and a comparison with the Kohistan arc. *Geophys. Res. Abs.*, **Vol 5** (EAE03-A-08308).

Varella, M.E., Clochiatti, R., Kurat, G., Schiano, P. (1999): Silicic glasses in hydrous and anhydrous mantle xenoliths from Western Victoria, Australia: at least two different sources. *Chemical Geol.*, **153**, 151-169.

Vernon, R.H. (2004): A practical guide to rock microstructure. Cambridge Univ. Press, 594 p.

Zhao, G.C., Wilde, S.A., Cawood, P.A., Lu, L.Z. (2000): Petrology and P-T path of the Fuping mafic granulites: implications for tectonic evolution of the central zone of the North China craton. *J. metamorphic Geol.*, **18**, 375-391.

Received 18 March 2004
Modified version received 22 February 2005
Accepted 13 May 2005